

# PGC1 $\alpha$ Expression Defines a Subset of Human Melanoma Tumors with Increased Mitochondrial Capacity and Resistance to Oxidative Stress

Francisca Vazquez,<sup>1,6</sup> Ji-Hong Lim,<sup>1,6</sup> Helen Chim,<sup>1</sup> Kavita Bhalla,<sup>2</sup> Geoff Girnun,<sup>2</sup> Kerry Pierce,<sup>3</sup> Clary B. Clish,<sup>3</sup> Scott R. Granter,<sup>4</sup> Hans R. Widlund,<sup>5</sup> Bruce M. Spiegelman,<sup>1</sup> and Pere Puigserver<sup>1,\*</sup>

<sup>1</sup>Department of Cancer Biology, Dana-Farber Cancer Institute and Department of Cell Biology, Harvard Medical School, Boston, MA 02115, USA

<sup>2</sup>Stewart Greenebaum Cancer Center, Department of Pathology, University of Maryland School of Medicine, Baltimore, MD 21201, USA

<sup>3</sup>Metabolite Profiling Initiative, Broad Institute of MIT and Harvard, 7 Cambridge Center, Cambridge, MA 02142, USA

<sup>4</sup>Department of Pathology

<sup>5</sup>Department of Dermatology

Harvard Skin Disease Research Center, Brigham and Women's Hospital, Boston, MA 02115, USA

<sup>6</sup>These authors contributed equally to this work

\*Correspondence: [pere\\_puigserver@dfci.harvard.edu](mailto:pere_puigserver@dfci.harvard.edu)

<http://dx.doi.org/10.1016/j.ccr.2012.11.020>

## SUMMARY

Cancer cells reprogram their metabolism using different strategies to meet energy and anabolic demands to maintain growth and survival. Understanding the molecular and genetic determinants of these metabolic programs is critical to successfully exploit them for therapy. Here, we report that the oncogenic melanocyte lineage-specification transcription factor MITF drives PGC1 $\alpha$  (*PPARGC1A*) overexpression in a subset of human melanomas and derived cell lines. Functionally, PGC1 $\alpha$  positive melanoma cells exhibit increased mitochondrial energy metabolism and reactive oxygen species (ROS) detoxification capacities that enable survival under oxidative stress conditions. Conversely, PGC1 $\alpha$  negative melanoma cells are more glycolytic and sensitive to ROS-inducing drugs. These results demonstrate that differences in PGC1 $\alpha$  levels in melanoma tumors have a profound impact in their metabolism, biology, and drug sensitivity.

## INTRODUCTION

Tumors reprogram their metabolism to meet increased energetic and anabolic demands. A frequent metabolic adaptation that cancer cells acquire is an increase in glucose uptake and aerobic glycolysis together with decrease in oxidative metabolism. It is clear, however, that there is not one single tumor-specific metabolic state, and tumors can utilize a variety of different metabolic strategies that have only now begun to be elucidated. For example, tumor cells are able to generate ATP through mitochondrial oxidation of fatty acids and amino acids, such as glutamine when glucose becomes limiting (Zaugg et al., 2011; Choo et al., 2010; Gao et al., 2009; Wise et al., 2008).

An increase in reactive oxygen species (ROS), due to an enhanced and unbalanced metabolic activity (Hanahan and Weinberg, 2011) is a common stressor to which tumors must adapt. This increased generation of ROS can play a dual role in the cancer phenotype. On one hand, it can play a tumorigenic role by stimulating cell proliferation and promoting genomic instability (Weinberg and Chandel, 2009). On the other hand, above a certain threshold, ROS can be toxic and induce cellular damage, leading to cell death (Trachootham et al., 2009; Diehn et al., 2009). Cancer cells develop adaptive responses against oxidative stress, often by upregulating their antioxidant-scavenging capacity. One clear example is the constitutive activation of the Keap1-Nrf2 pathway in squamous cell carcinomas, either

### Significance

Tumor cells reprogram a variety of central metabolic and bioenergetic pathways to maintain exacerbated growth and survival rates. The identification of the genetic factors responsible for specific metabolic programs is key to exploit this reprogramming for cancer therapy. Here, we show that, in melanomas, overexpression of the transcriptional coactivator PGC1 $\alpha$ , a key regulator of mitochondrial respiration, metabolically defines melanoma tumors with high bioenergetic and ROS detoxification capacities. These metabolic capacities allow PGC1 $\alpha$ -positive melanomas higher rates of survival under oxidative stress compared to PGC1 $\alpha$ -negative melanomas. Our results underscore how different metabolic vulnerabilities defined by PGC1 $\alpha$  expression could be therapeutically exploited to treat melanoma tumors.

by activating mutations in *Nrf2* or through inactivating mutations in *KEAP1* (an Nrf2 cytoplasmic repressor) (Padmanabhan et al., 2006; Singh et al., 2006; Shibata et al., 2008; Ohta et al., 2008). Whereas some of these components of the oxidative stress response have been identified in cancer cells, it is likely that key regulators in this response that contribute to tumorigenesis are still missing.

PPARGC1A, named hereafter PGC1 $\alpha$ , is part of a small family of transcriptional coactivators, including PGC1 $\beta$  and PRC, that promote mitochondrial biogenesis and respiration (Puigserver and Spiegelman, 2003; Scarpulla, 2011). PGC1 $\alpha$  is the best studied, particularly in brown fat, skeletal and cardiac muscle, liver, and fat tissues, where it is a key regulator of mitochondrial mass, thermogenic programs, and adaptation to fasting conditions (Kelly and Scarpulla, 2004). PGC1 $\alpha$  can also potentially reduce generation of mitochondrial-driven ROS (St-Pierre et al., 2006). PGC1 $\alpha$  is typically expressed at low levels under normal conditions and is strongly induced and activated in response to increased metabolic and energetic demands in highly metabolic tissues. For example, exercise increases PGC1 $\alpha$  levels in skeletal muscle, where it induces mitochondrial biogenesis and oxidative capacity (Handschin et al., 2007). Cold exposure rapidly increases PGC1 $\alpha$  levels in brown/beige adipose tissue to program a thermogenic response based on mitochondrial function (Puigserver et al., 1998). In liver, fasting increases PGC1 $\alpha$  to induce fatty acid oxidation, hepatic glucose production, and ketogenesis (Rhee et al., 2003). In many of these cell types, the cyclic AMP (cAMP) pathway plays a central role through the activation of a cAMP response element binding protein (CREB) response element at the *PGC1 $\alpha$*  promoter (Herzig et al., 2001). Other signals contribute to increases in *PGC1 $\alpha$*  gene expression, such as calcium signaling and MEF2 transcriptional activity in skeletal muscle (Lin et al., 2002). It is unknown, however, whether and how oncogenic signals impact PGC1 $\alpha$  expression and what are the metabolic and growth consequences this might cause to the tumor phenotype.

## RESULTS

### A Subset of Human Melanoma Tumors Expresses High Levels of PGC1 $\alpha$ and Mitochondrial Genes of Oxidative Metabolism

Given the central role of PGC1 $\alpha$  in oxidative metabolism and ROS detoxification in a variety of tissues (Puigserver and Spiegelman, 2003; Kelly and Scarpulla, 2004; Fernandez-Marcos and Auwerx, 2011; St-Pierre et al., 2006), we hypothesized that PGC1 $\alpha$  could be aberrantly activated in some tumors, thereby conferring them an adaptive advantage. Since *PGC1 $\alpha$*  is strongly regulated at the messenger RNA (mRNA) level, publicly available gene expression databases were surveyed. In several data sets, a subset of melanoma tumors and melanoma-derived cell lines expressed very high relative levels of *PGC1 $\alpha$*  mRNA. Figures 1A and S1A (available online) show the relative *PGC1 $\alpha$*  mRNA levels from 56 melanoma tumors (GSE7553) (Riker et al., 2008) and 82 short-term melanoma cultures (Lin et al., 2008). Levels of 10.7% for Riker melanoma data set and 8.4% for short-term melanoma cultures showed *PGC1 $\alpha$*  expression levels that are at least one standard deviation above the average. To assess if the high *PGC1 $\alpha$*  levels in

these melanoma tumors were associated with its known metabolic gene expression program, we used Gene Set Enrichment Analysis (GSEA) to find gene expression signatures that correlated with *PGC1 $\alpha$*  expression. Consistent with previous and established *PGC1 $\alpha$*  targets in skeletal muscle cells (Mootha et al., 2003), gene expression sets of mitochondrial genes, energy metabolism, and estrogen-related receptor alpha target genes were all significantly correlated with *PGC1 $\alpha$*  expression in both melanoma tumors and short-term melanoma cultures (Table 1; Table S1). Using an additional data set of metastatic melanoma tumors with clinical outcome data (Bogunovic et al., 2009), we found that tumors expressing high *PGC1 $\alpha$*  levels were associated with lower survival (long-rank p value 0.0230) compared to low *PGC1 $\alpha$* -expressing tumors (Figure 1B). The high and low expressing tumors were defined by selecting the top and bottom 25% *PGC1 $\alpha$*  expressing tumors. Other clinical parameters were not affected (Figure S1B). The overexpression results were validated using patient-derived long-term melanoma cell lines. Remarkably, all melanoma cell lines tested fell into two categories with very high levels (*PGC1 $\alpha$*  positive) or undetectable or very low levels (*PGC1 $\alpha$*  negative) of *PGC1 $\alpha$*  mRNA (Figure 1C) and protein (Figure 1D). *PGC1 $\alpha$* -positive cell lines had elevated levels of mitochondrial respiratory chain proteins from all different complexes tested (Figure 1D). These results suggest that *PGC1 $\alpha$*  induces a mitochondrial metabolism gene expression program in these tumors and tumor-derived cell lines.

To confirm that *PGC1 $\alpha$*  was driving the mitochondrial metabolism gene expression signature, we used lentiviral small hairpin RNA (shRNA) to reduce its expression in a *PGC1 $\alpha$* -positive melanoma cell line (A375P) and performed gene-expression microarray followed by GSEA analysis. Similar gene expression sets of mitochondrial energy metabolism as the ones found in melanoma tumors and short-term melanoma cultures were enriched in control versus *PGC1 $\alpha$*  knockdown cell lines (Figure 1E; Table S2). Some of the targets were confirmed using quantitative PCR (qPCR) in A375P and two other *PGC1 $\alpha$* -positive melanoma cell lines (MeWo and G361) (Figure 1F). As expected, downregulation of mitochondrial genes in *PGC1 $\alpha$* -depleted A375P cells translated into decreases of protein levels. Several components of the oxidative phosphorylation complex were substantially decreased in *PGC1 $\alpha$*  knockdown cells, particularly proteins that are part of Complex I and Complex IV (Figure 1G). *PGC1 $\alpha$*  expression was also sufficient to induce this mitochondrial program. Modest ectopic expression of *PGC1 $\alpha$*  in a *PGC1 $\alpha$* -negative cell line (A375, a metastatic clone derived from A375P) increased mitochondrial gene targets and protein levels (Figures S1C and S1D). We then compared the levels of *PGC1 $\alpha$*  between nontransformed melanocytes and melanoma cells. The relative levels of *PGC1 $\alpha$*  mRNA expression were measured in cultured immortal primary melanocytes and in a *PGC1 $\alpha$* -positive and negative melanoma cell lines. *PGC1 $\alpha$*  mRNA expression levels in primary melanocytes were higher than *PGC1 $\alpha$* -negative melanoma cells but dramatically lower than *PGC1 $\alpha$* -positive melanoma cells (Figure S1E). Together, these results indicate that *PGC1 $\alpha$*  is overexpressed in a subset of melanoma tumors and drives a mitochondrial gene expression program.

Interestingly, the overexpression of *PGC1 $\alpha$*  and correlation with oxidative metabolism is not only present in melanomas.

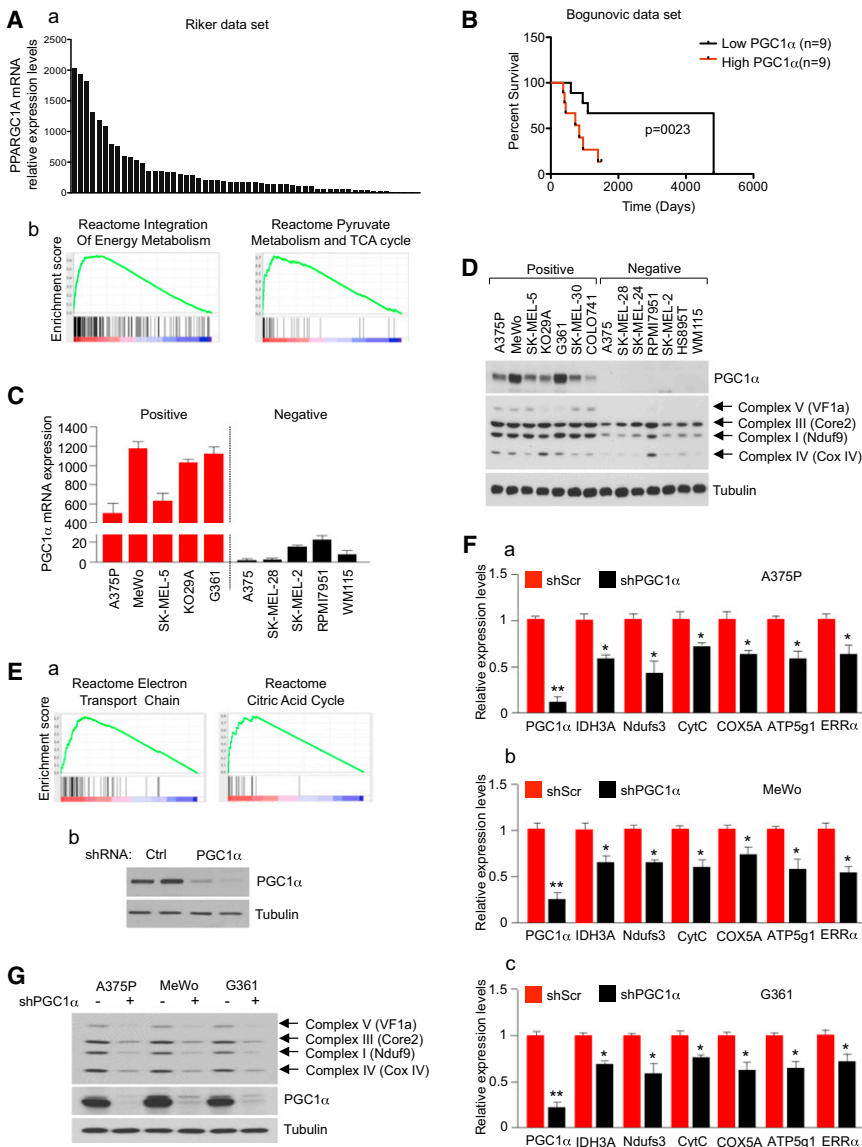


**Figure 1. PGC1 $\alpha$  Drives the Expression of a Mitochondrial Respiration Program in a Subset of Human Melanoma Tumors and Derived Cell Lines**

(A) (a) Relative expression levels of *PGC1 $\alpha$*  in 56 melanoma tumors included in the data set GSEA7553 (Riker et al., 2008). (b) Plots for two of the top gene sets from GSEA analysis of genes positively correlated with *PGC1 $\alpha$*  expression.

(B) Kaplan-Meier survival curves for metastatic melanoma tumors with high and low *PGC1 $\alpha$*  expression from data set GSE19232 (Bogunovic et al., 2009). Survival curves for the 18 metastatic melanoma patients with tumors expressing the 25% highest and lowest *PGC1 $\alpha$*  levels were calculated using Kaplan-Meier analysis with test of statistical significance using the Mantel-Cox log-rank test. The long-rank p value was 0.0230.

(C) *PGC1 $\alpha$*  mRNA expression levels in ten human melanoma cell lines. mRNA levels were quantified using qRT-PCR. Values represent mean  $\pm$  SD of two independent experiments performed in triplicate.

(D) Protein levels of *PGC1 $\alpha$*  and mitochondrial respiration-associated proteins in human melanoma cell lines.

(E) (a) Plots for two of the top gene sets of the GSEA analysis in control versus *PGC1 $\alpha$*  knocked down A375P cells. (b) *PGC1 $\alpha$*  protein levels in the control and *PGC1 $\alpha$*  knocked down cells.

(F) mRNA levels of *PGC1 $\alpha$*  mitochondrial target genes measured using qRT-PCR analysis after *PGC1 $\alpha$*  knockdown in *PGC1 $\alpha$* -positive cell lines: (a) A375P; (b) MeWo; and (c) G361. Values represent mean  $\pm$  SD of three independent experiments performed in triplicate. \* $p < 0.05$  and \*\* $p < 0.01$ .

(G) Protein expression levels of mitochondrial respiration-associated proteins and *PGC1 $\alpha$*  in A375P stably expressing a control or *PGC1 $\alpha$*  shRNA.

See also Figure S1 and Tables S1–S3.

We found that levels of *PGC1 $\alpha$*  expression in lung adenocarcinoma cell lines also correlate with an oxidative metabolism signature (Figure S1; Table S3).

### MITF Expression in Human Melanoma Cells Drives High Levels of *PGC1 $\alpha$* Gene Expression

In order to identify the key factors responsible for the high levels of *PGC1 $\alpha$*  expression in melanoma, we used publicly available data on gene expression, copy number, and mutations from the Cancer Cell Line Encyclopedia (CCLE) database (<http://www.broadinstitute.org/ccle>) (Barretina et al., 2012). We found no correlation between *PGC1 $\alpha$*  copy number levels and gene expression. Only one melanoma cell line (SK-MEL1)—out of 60 melanoma cell lines with copy number data available at the time (Figure S2A, data from the CCLE database)—was found to have *PGC1 $\alpha$*  amplification, suggesting that amplification is not a common mechanism to increase *PGC1 $\alpha$*  expression levels. Since p53 has been shown to negatively regulate *PGC1 $\alpha$*  levels

(Sahin et al., 2011; Sen et al., 2011), we searched if there was an association between p53 mutation status and *PGC1 $\alpha$*  expression, but no correlation was found in 60 cell lines with expression and mutation status data. Similarly, there was no correlation with BRAF mutations status (Figure S2B). The Riker melanoma data set was classified by their *PGC1 $\alpha$*  expression levels to identify genes that were upregulated in high *PGC1 $\alpha$*  versus low *PGC1 $\alpha$* -expressing tumors (Figure 2A). Intriguingly, among the top classifying genes identified was microphthalmia-associated transcription factor (*MITF*), a melanocyte-lineage transcription factor and bona fide melanoma oncogene (Garraway et al., 2005; Yokoyama et al., 2011; Bertolotto et al., 2011). Similar results were obtained comparing high- versus low-expressing *PGC1 $\alpha$*  melanoma cell lines. Furthermore, the levels of several *MITF* downstream target genes, such as *SLC45A2*, *CDK2*, *PMEL*, *TYR*, *TYRP1*, *MLANA*, and *DCT*, were also differentially expressed (Figure 2B, data from the CCLE database). Hence, within both melanoma specimens and melanoma cell lines, the

**Table 1. GSEA of Genes Ranked by Positive Correlation with PGC1 $\alpha$  Expression in Melanoma Tumors**

Name	NES	FDR q-value
Reactome_integration_of_energy_metabolism	2.15	0.02
Reactome_glucose_regulation_of_insulin_secretion	2.08	0.03
Reactome_regulation_of_insulin_secretion	2.09	0.04
Reactome_pyruvate_metabolism_and_TCA_cycle	1.94	0.1
Reactome_citric_acid_cycle	1.88	0.13
Reactome_peroxisomal_lipid_metabolism	1.88	0.16
Reactome_electron_transport_chain	1.86	0.13

Gene expression of 56 melanoma tumors extracted from the GSEA7553 data set (Riker et al., 2008) was ranked for positive correlation with PGC1 $\alpha$  expression and analyzed with the GSEA algorithm using the reactome gene sets; the significant ( $q < 0.25$ ) gene sets ranked by normalized enrichment score are shown. NES, normalized enrichment score.

expression levels of PGC1 $\alpha$  correlated with MITF levels, indicating that they may be affecting each other in an epistatic manner. To forward this notion, we analyzed mRNA and protein levels of MITF in five PGC1 $\alpha$ -positive and five PGC1 $\alpha$ -negative cell lines. We found that both the mRNA and protein levels were higher in PGC1 $\alpha$ -positive cell lines (Figure 2C). Interestingly, one of the outlier cell lines (SK-MEL-28) that expresses high levels of MITF but is PGC1 $\alpha$ -negative expresses high levels of PGC1 $\beta$ .

Based on these data, we investigated if MITF was a causal driver for the high levels of PGC1 $\alpha$  gene expression. Hence, we used lentiviral shRNA to reduce endogenous MITF levels in three PGC1 $\alpha$ -positive melanoma cell lines (A375P, G361, and SK-MEL5) and found that it strongly downregulated PGC1 $\alpha$  both at the mRNA and protein levels (Figures 2D and 2E). Notably, PGC1 $\alpha$  expression levels were suppressed even further than the known MITF target TYR. Moreover, PGC1 $\alpha$  protein levels were almost undetectable after MITF knockdown. As expected, MITF knockdown-induced PGC1 $\alpha$  downregulation resulted in decrease of PGC1 $\alpha$  targets, including mitochondrial genes (Figure S2C). These results indicate that MITF is necessary to maintain high levels of PGC1 $\alpha$  expression in PGC1 $\alpha$ -positive melanoma cell lines.

Next we investigated whether MITF was sufficient to induce PGC1 $\alpha$  expression in melanoma cell lines. Hence, ectopic expression of MITF using retroviral transduction in A375, a PGC1 $\alpha$ -negative cell line, caused induction of PGC1 $\alpha$  mRNA levels, including PGC1 $\alpha$  targets, comparable to the known MITF target genes, TYR and DCT (Figure 2F). Because MITF is a transcription factor, it could directly bind the upstream regulatory promoter of PGC1 $\alpha$ , as this region contains several E-boxes sequences (Figure S2D). Transfection of HEK293T cells with MITF induced a 2Kb PGC1 $\alpha$  promoter-driving luciferase that was dependent on both E-boxes (Figure 2Ga). Conversely, MITF knockdown experiments in A375P cells reduced the activity of this promoter (Figure 2Gb). In addition, chromatin immunoprecipitation (ChIP) assays showed that endogenous MITF is bound to the PGC1 $\alpha$  promoter (Figure 2H), consistent with previously reported ChIP sequencing data set (Strub et al., 2011; Figure S2E).

Gene expression profiling analysis of melanoma tumors has previously identified two expression signatures associated with proliferative or invasive phenotype. MITF expression was higher in melanoma samples with the proliferative signature and lower in samples with an invasive signature (Hoek et al., 2008). Consistently, we found that melanoma tumors with high PGC1 $\alpha$  levels also correlated with the proliferative signature (Figure S2F).

Collectively, these results indicate that MITF is necessary and contributes to the high levels of PGC1 $\alpha$  expression found in a subset of human melanoma cells.

### PGC1 $\alpha$ Defines the Metabolic State of Melanoma Cells

To test whether PGC1 $\alpha$  expression levels drive the metabolic program of melanoma cells, we compared key cellular metabolic and bioenergetic parameters between PGC1 $\alpha$ -positive and negative melanoma cells. PGC1 $\alpha$ -positive cells exhibited substantial increased basal and maximal oxygen consumption rates (Figure 3A). Additionally, the respiration reserve capacity, calculated by subtracting the basal to the maximal respiration capacity, was significantly higher in PGC1 $\alpha$ -expressing melanoma cells. Glucose uptake was slightly decreased in PGC1 $\alpha$ -positive cells that paralleled diminished levels of secreted lactate compared to PGC1 $\alpha$ -negative cells (Figure 3B). Consistent with glycolytic metabolism generating lower ATP levels compared to oxidative metabolism, intracellular ATP levels of PGC1 $\alpha$ -negative melanoma cell lines were reduced (Figure 3B). These differences in metabolic parameters were caused by PGC1 $\alpha$  expression. Depletion of PGC1 $\alpha$  levels in A375P largely recapitulated the metabolic and bioenergetic patterns of PGC1 $\alpha$ -negative cells, e.g., decreased in basal, maximal, and reserved oxygen consumption rate (OCR) and intracellular ATP levels, decreased glucose uptake, and increased lactate production (Figures 3C and 3D). Metabolomic analysis showed that shRNA PGC1 $\alpha$  cells had increased glycolytic but decreased tricarboxylic acid (TCA) intermediates (Figure S3). In addition, a modest increase in PGC1 $\alpha$  levels through forced expression (Figure S1C) in a PGC1 $\alpha$ -negative cell line resulted in a reversal of these metabolic parameters (Figure 3E). In summary, these results indicate that cells with undetectable levels of PGC1 $\alpha$  have lower rates of mitochondrial oxidative metabolism but elevated rates of glycolysis and lactate production consistent with a more pronounced glycolytic “Warburg” state. In contrast, PGC1 $\alpha$ -positive cells have the reversed metabolic phenotype, leading to an elevated cellular energetic state.

### PGC1 $\alpha$ -Positive Melanoma Cells Are Dependent on PGC1 $\alpha$ for Survival and Tumor Progression

Given the central role of PGC1 $\alpha$  in the metabolic and energetic state of a subset of melanoma cells with high expression levels, we investigated whether these cells may have become dependent on PGC1 $\alpha$  for survival. Thus, we suppressed the expression of PGC1 $\alpha$  in five positive cell lines and measured its effect on cell viability. Figure 4A shows that knockdown of PGC1 $\alpha$  significantly decreased cell number. As expected, knockdown of PGC1 $\alpha$  had no significant effect on PGC1 $\alpha$ -negative cells. As an additional control, we tested the effect of RPS6 knockdown in a PGC1 $\alpha$ -positive and negative cell line and observed a similar effect of decreased cell number in both PGC1 $\alpha$ -positive and negative cell lines (Figure S4A). Overexpression of PGC1 $\alpha$ , similar to

MITF, was not sufficient to induce proliferation in PGC1 $\alpha$ -negative melanoma cells (Figures S4B–S4D) underscoring the context dependency of the effects.

We next investigated the mechanism responsible for the reduced cell number after PGC1 $\alpha$  knockdown. PGC1 $\alpha$  knockdown resulted in a more than 3-fold induction in the percentage of apoptotic cells in two PGC1 $\alpha$ -positive cell lines (A375P and MeWo) but not in a negative cell line (A375) (Figure 4B). This apoptosis was mediated through the intrinsic pathway, as caspases 9 and 3 but not 8 were activated in PGC1 $\alpha$ -depleted cells. Other apoptotic markers, including cleavage of poly (ADP-ribose) polymerase (PARP), was also induced in PGC1 $\alpha$  knockdown cells (Figure 4C). The apoptotic effect was largely reversed by overexpression of PGC1 $\alpha$ , indicating that it is a result of PGC1 $\alpha$  depletion (Figure 4D). To further support the involvement of caspases, the inhibitor Q-VD-OPH significantly reduced the number of cells entering apoptosis (Figure 4E). These results indicate that suppression of PGC1 $\alpha$  activates the intrinsic mitochondrial apoptotic pathway and strongly suggest that PGC1 $\alpha$ -positive melanoma cells have become dependent on PGC1 $\alpha$  for survival.

#### **PGC1 $\alpha$ Suppression Results in a Reduction of ROS Detoxification Genes and Increase in ROS Levels Leading to Apoptosis**

The fact that the intrinsic apoptotic pathway was activated in PGC1 $\alpha$ -depleted cells suggested that the mitochondria was involved in the induction of apoptosis. One of the mechanisms by which mitochondrial failure causes apoptosis is through the loss of membrane potential and generation of ROS (Tait and Green, 2010). Consistent with induction of this process, knockdown of PGC1 $\alpha$  in A375P cells showed a strong decrease in mitochondrial membrane potential as measured using J-aggregation fluorescent assay (Figure 5A). Intracellular concentrations of ROS were significantly increased in PGC1 $\alpha$ -depleted cells (Figure 5B), and this was associated with a decrease in glutathione (GSH), cystathionine, and 5-adenosylhomocysteine levels (Figure 5C). Importantly, elevated ROS levels were necessary to mediate apoptosis in PGC1 $\alpha$  knockdown cells, because two different antioxidants, N-acetyl-L-cysteine (NAC) and Trolox, largely suppressed caspase and PARP cleavages and the number of apoptotic cells (Figure 5D).

To determine whether ROS detoxification genes decrease in PGC1 $\alpha$ -depleted cells and might contribute to apoptosis, we analyze the microarray data described in Figure 1. Consistent with previous data in non-transformed cells (St-Pierre et al., 2006), a set of genes involved in the ROS detoxification, including different glutathione synthase enzymes, thioredoxins, glutaredoxin, peroxiredoxins, and SOD2, were decreased in PGC1 $\alpha$  knockdown cells. These results were confirmed using qPCR of several of these genes (Figure 5E). SOD2 protein levels were substantially decreased in PGC1 $\alpha$ -depleted melanoma cells (Figure 5F). Moreover, ectopic expression of PGC1 $\alpha$  in A375 increased ROS detoxification genes (Figure 5G). These data supports a key role for PGC1 $\alpha$  in activating the ROS detoxification gene program to maintain melanoma cell survival.

As we have showed that PGC1 $\alpha$  is a target of MITF, we next investigated the role of PGC1 $\alpha$  downstream of MITF in promoting survival and proliferation. Overexpression of PGC1 $\alpha$

could partially overcome the effects of knockdown MITF on DNA damage and increase of p27 levels (Figure S5A). In addition, treatment of MITF-depleted cells with the antioxidant NAC partially blocked the apoptotic effects (Figure S5B). Together, these results suggest that downregulation of PGC1 $\alpha$  contributes to the phenotypic effects of MITF knockdown in PGC1 $\alpha$ -expressing cells.

#### **Depletion of Several PGC1 $\alpha$ Respiratory Chain Targets Mimic the Metabolic and ROS-Dependent Apoptotic Effects of PGC1 $\alpha$ Suppression**

The reduction in ROS detoxification genes and GSH levels could be one of the mechanisms by which depletion of PGC1 $\alpha$  in melanoma cells induces intracellular ROS levels. However, defects in mitochondrial bioenergetic function are also known to generate toxic ROS levels. Thus, to understand how PGC1 $\alpha$  deficiency caused ROS-mediated apoptosis, we tested whether knockdown of different proteins of the mitochondrial respiratory complexes, which are PGC1 $\alpha$  targets, produced similar metabolic and apoptotic defects as PGC1 $\alpha$  depletion. Therefore, Ndufs3, Cox5a, and ATP5b were efficiently knocked down in A375P melanoma cells (Figure 6A). Individual depletion of these three mitochondrial proteins caused a similar metabolic phenotype as PGC1 $\alpha$  knockdown cells, leading to decreases in oxygen consumption and increases in glucose uptake and lactate secretion (Figures 6B and 6C). Consistent with an increase in intracellular ROS levels in these cells, GSH levels were also decreased (Figure 6D). Moreover, increased ROS concentrations caused by depletion of these mitochondrial proteins lead to increased cleavage of proapoptotic proteins (Figures 6E and 6F). To support the role of ROS mediating cell death, treatment with antioxidants NAC and Trolox largely prevented PARP cleavage (Figure 6G). Together, these results suggest that PGC1 $\alpha$ -positive melanoma cells are highly sensitive to the induction of ROS due, at least in part, to the disruption of the mitochondria respiratory complex.

#### **PGC1 $\alpha$ Protects against ROS-Induced Apoptosis in Human Melanoma Cells and Tumors**

The increased ROS levels in cancer cells makes them more dependent in their antioxidant capacity for cell survival, a principle that is exploited by anticancer drugs, such as piperlongumine or phenethyl isothiocyanate (PEITC). In fact, transformed cells have been shown to be exquisitely more sensitive to ROS-inducing drugs than nontransformed cells (Trachootham et al., 2006; Raj et al., 2011). Based on the results presented above that PGC1 $\alpha$  controls the antioxidant capacity affecting cell survival, we investigated if PGC1 $\alpha$ , by reducing ROS levels and enhancing the antioxidant capacity, could influence the sensitivity to ROS-inducing drugs in melanoma cells. Depletion of PGC1 $\alpha$  in A375P cells enhanced their sensitivity to apoptosis induced by H<sub>2</sub>O<sub>2</sub>, PEITC, or piperlongumine, all of which are known to increase intracellular ROS concentrations (Trachootham et al., 2006; Raj et al., 2011). These effects were not generalized to all drugs, as the B-Raf inhibitor PLX4032 had similar effects in PGC1 $\alpha$  control or knockdown A375P cells (Figures 7A and S6A). Furthermore, similar effects on the sensitivity to these compounds were observed after knockdown of several mitochondrial proteins (Ndufs3, Cox5a, and ATP5b)

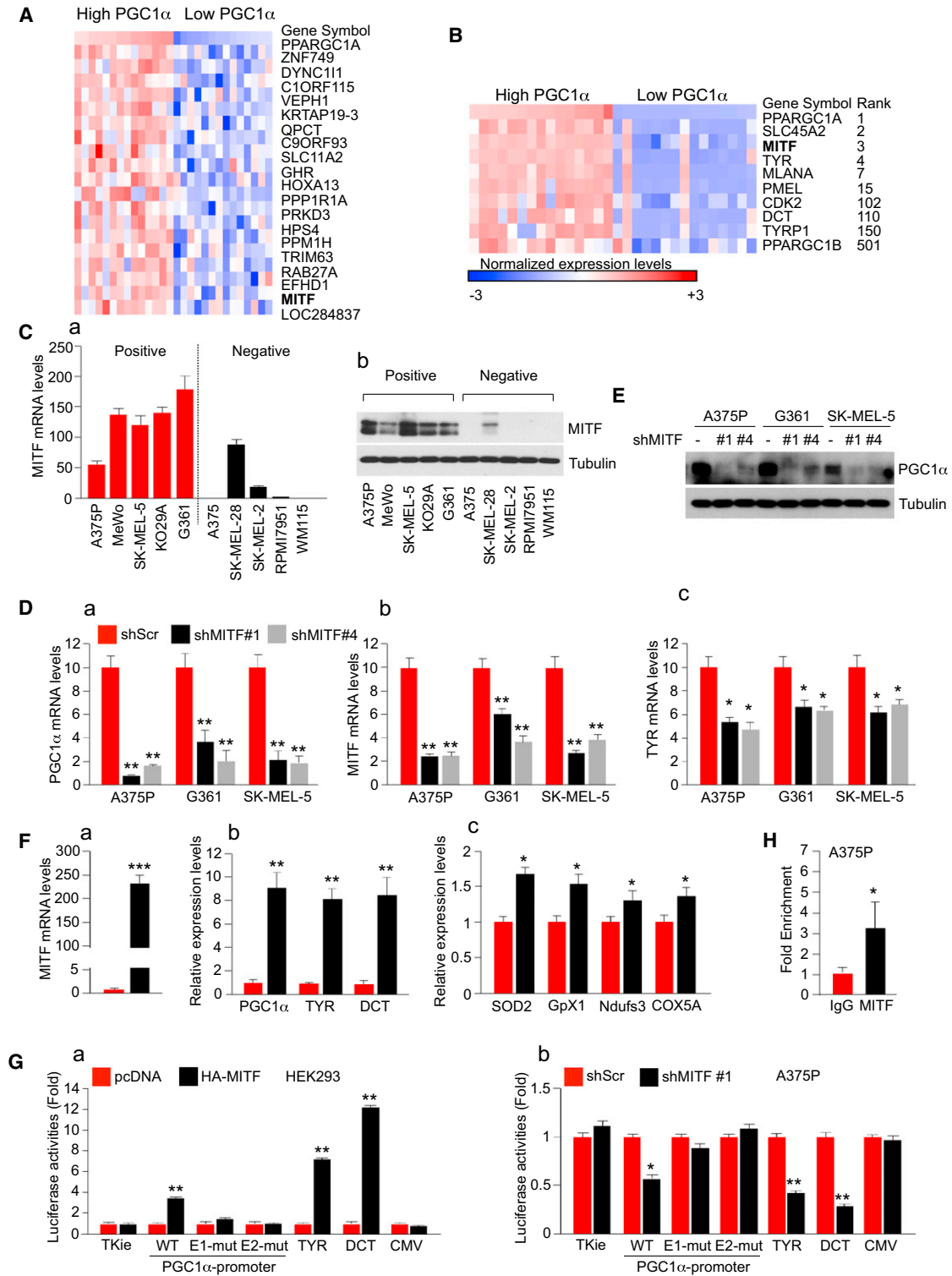


**Figure 2. MITF Is Necessary to Maintain High Levels of PGC1 $\alpha$  Gene Expression in Melanoma Cells**

(A) Heat map of the top 20 genes differentially expressed between the top and the bottom 25% of melanoma samples ranked by PGC1 $\alpha$  expression levels. Expression data were extracted from the GSE7553 data set. The gene list shown is ranked by signal to noise.

(B) Heat map of selected differentially expressed genes between the top and the bottom 25% of melanoma samples ranked by PGC1 $\alpha$  expression levels. Expression data were extracted from the CCLE database. The rank of the genes by signal to noise is shown.

(C) (a) MITF mRNA and (b) protein expression levels in five PGC1 $\alpha$ -positive and five PGC1 $\alpha$ -negative melanoma cell lines. Values represent mean  $\pm$  SD of three independent experiments performed in triplicate.

(legend continued on next page)

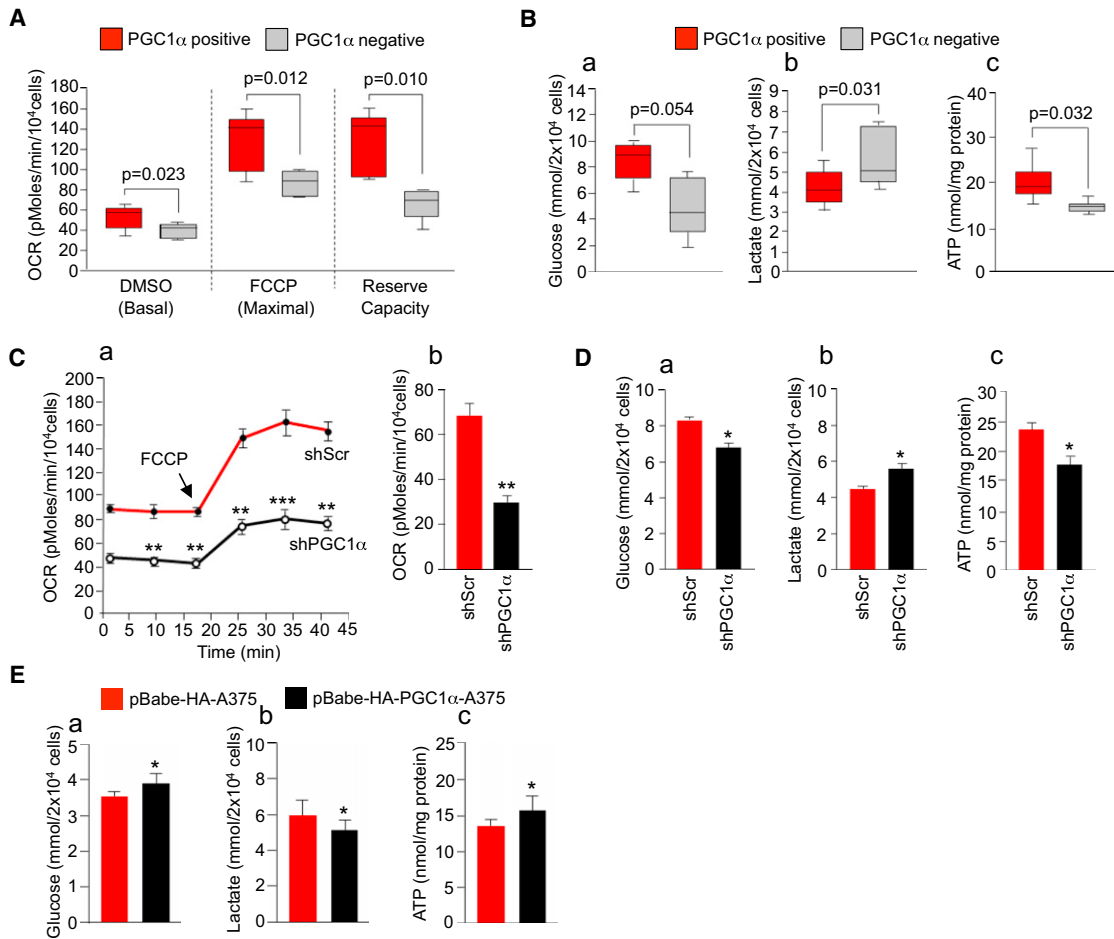


**Figure 3. PGC1 $\alpha$  Defines the Metabolic and Energetic Program of Human Melanoma Cells**

(A) Basal and maximal oxygen consumption rates (OCR) in PGC1 $\alpha$ -positive and negative cells measured in DMSO control or FCCP-treated cells. The reserve capacity was calculated by subtracting the basal from the maximum OCR. Values of two independent experiments performed in quadruplicate were averaged. The whiskers in the box plots represent the maximum and the minimum value.

(B) (a) Glucose (in the culture media), (b) lactate (in the culture media), and (c) intracellular ATP levels of PGC1 $\alpha$ -positive compared to PGC1 $\alpha$ -negative cells. Values of three independent experiments performed in duplicate were averaged. The whiskers in the box plots represent the maximum and the minimum value.

(C) (a) Real-time measurement of basal and maximal (after addition of FCCP) OCR and (b) basal OCR in control and PGC1 $\alpha$  knockdown cells. Values represent mean  $\pm$  SD of two independent experiments performed in quadruplicate. \*\* $p < 0.01$  and \*\*\* $p < 0.001$ .

(D) (a) Glucose (in the culture media), (b) lactate (in the culture media), and (c) intracellular ATP levels in control and PGC1 $\alpha$  knockdown cells. Values represent mean  $\pm$  SD of three independent experiments performed in duplicate. \* $p < 0.05$ .

(E) (a) Glucose (in the culture media), (b) lactate (in the culture media), and (c) intracellular ATP levels in cells overexpressing PGC1 $\alpha$ . A375 cells stably expressing HA-PGC1 $\alpha$  were used. Values represent mean  $\pm$  SD of three independent experiments performed in duplicate. \* $p < 0.05$ .

See also Figure S3.

(Figure 7A). Consistent with these results, piperlongumine had a more potent effect, inducing apoptosis in PGC1 $\alpha$ -negative cells (Figures 7B and 7C). Furthermore, ROS levels after piper-

longumine treatment were higher in four out of the five PGC1 $\alpha$ -negative compared to five PGC1 $\alpha$ -positive cell lines tested (Figures 7D and S6B). To further support the role of

(D) qPCR analysis of (a) PGC1 $\alpha$ , (b) MITF targets, and (c) TYR in shRNA MITF melanoma cell lines. Values represent mean  $\pm$  SD of three independent experiments performed in triplicate. \* $p < 0.05$  and \*\* $p < 0.01$ .

(E) Western blot analysis of PGC1 $\alpha$  protein expression levels in control and MITF knockdown melanoma cell lines.

(F) qPCR analysis of (a) MITF, (b) MITF targets, and (c) PGC1 $\alpha$  target mRNAs in A375 melanoma cells ectopically expressing MITF. Values represent mean  $\pm$  SD of two independent experiments performed in triplicate. \* $p < 0.05$ , \*\* $p < 0.01$ , and \*\*\* $p < 0.001$ .

(G) PGC1 $\alpha$  promoter luciferase analysis using transient transfection with the indicated plasmids performed in (a) 293 and (b) A375P cells. Values represent mean  $\pm$  SD of two independent experiments performed in triplicate. \* $p < 0.05$  and \*\* $p < 0.01$ . A representation of the construct is shown in Figure S2D.

(H) ChIP analysis at the PGC1 $\alpha$  promoter in A375P cells using an antibody against MITF and immunoglobulin G (IgG) as a control. Values represent mean  $\pm$  SD of two independent experiments performed in triplicate. \* $p < 0.05$ .

See also Figure S2.

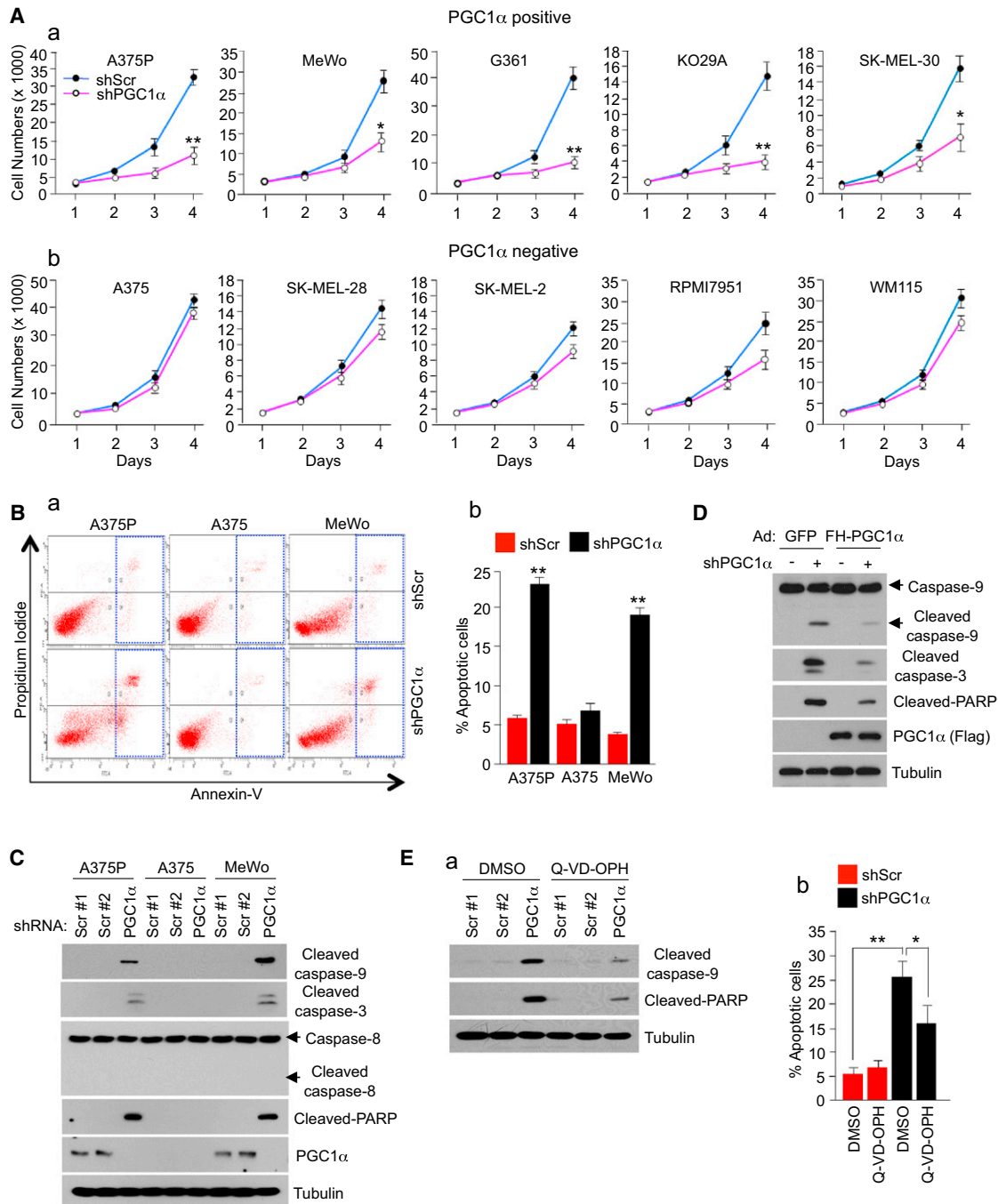


**Figure 4. PGC1 $\alpha$  Is Essential for Survival in Human Melanoma Cells**

(A) Cell number analysis after PGC1 $\alpha$  knockdown in (a) PGC1 $\alpha$ -positive and (b) PGC1 $\alpha$ -negative melanoma cells measured for 4 days after puromycin selection. Values on the graph represent mean  $\pm$  SD of three independent experiments performed in quadruplicate. \* $p < 0.05$  and \*\* $p < 0.01$ .

(B) (a) Annexin V analysis of apoptosis after PGC1 $\alpha$  knockdown in PGC1 $\alpha$ -positive melanoma cells. (b) Quantitation of the percentage of apoptotic cells. Data represent mean  $\pm$  SD of three independent experiments performed in triplicate. \*\* $p < 0.01$ .

(C) Western blot analysis of cleaved apoptotic proteins in PGC1 $\alpha$  knocked down and control melanoma cells.

(D) Western blot analysis of cleaved apoptotic proteins in cells expressing ectopic PGC1 $\alpha$  in control and PGC1 $\alpha$  knockdown A375P melanoma cells.

(E) Apoptosis measured by (a) western blot analysis of caspases and PARP cleavages or (b) Annexin V assays in PGC1 $\alpha$  knocked down and control A375P cells treated with 20  $\mu$ M Q-VD-OPH (a pan-caspase inhibitor) for 2 days. Values on the graph represent mean  $\pm$  SD of three independent experiments performed in triplicate. \* $p < 0.05$  and \*\* $p < 0.01$ .

See also Figure S4.



PGC1 $\alpha$ -mediating resistance to ROS-induced apoptosis, ectopic expression of PGC1 $\alpha$  in PGC1 $\alpha$ -negative cell lines prevented piperlongumine-induced cleavage of caspase 9 and PARP (Figure 7E).

Finally, to evaluate the impact of PGC1 $\alpha$  depletion on tumor growth, subcutaneous injections of control and PGC1 $\alpha$ -depleted A375P cells were performed in nude mice and the size of the resulting tumors was measured. As shown in Figure 8A, there was a significant reduction in tumor size in PGC1 $\alpha$ -depleted cells, suggesting that PGC1 $\alpha$  is important for tumor progression. Importantly, piperlongumine treatment for 7 days had a greater reduction of tumor volume of xenografts derived from PGC1 $\alpha$  knockdown cells compared to control xenografts. The magnitude of these effects correlated with induction of apoptotic markers in these tumors (Figure 8B). The growth of these tumors did not affect body weight (Figure 8C). Collectively, these data suggest that PGC1 $\alpha$  expression confers resistance to drugs that induce intracellular ROS levels in melanoma cells and tumors.

## DISCUSSION

Cancer cells reprogram their metabolism to meet anabolic and energetic demands necessary for growth and survival. It is becoming clear, however, that tumor cells do not employ a single strategy to accomplish this, as cancers can choose from a variety of metabolic programs to meet their demands. Here, we provide a clear example of this metabolic reprogramming heterogeneity by showing that cells derived from the one tumor type can have profound differences in their metabolic state. In melanomas, expression levels of PGC1 $\alpha$  metabolically define two types of tumors with different bioenergetic and ROS detoxification capacities, thereby affecting the ability to survive under oxidative stress. It is conceivable that, in certain low nutrient conditions, elevated mitochondrial capacity might be more efficient to generate ATP necessary for survival without compromising anaerobic reactions to support cell growth.

Our findings show that a subset of melanoma cells acquire high levels of PGC1 $\alpha$  that depend on an increased activity of the melanoma oncogene *MITF*. This would confer a selective advantage to melanocytic tumor cells by providing a strong protection against oxidative damage. A large subset of melanoma tumors has very low or undetectable levels of PGC1 $\alpha$  that, to a large extent, overlaps with low levels of *MITF*. These less differentiated tumors use a different metabolic strategy of increased glycolysis for growth and survival. It is also possible that melanoma tumors transit through different states during tumor progression with high or low expression levels of PGC1 $\alpha$ . In fact, we provide here an example of this possibility: the PGC1 $\alpha$ -negative melanoma cell line A375 was derived from a metastatic tumor produced by the PGC1 $\alpha$ -positive parental cell line A375P (Clark et al., 2000). It is likely that A375 cells lost their melanocytic differentiation state, since they express very low levels of *MITF* and differentiation markers. Concomitant to this loss of differentiation, they became *MITF* and PGC1 $\alpha$  independent for tumor progression. Thus, similar to *MITF*, PGC1 $\alpha$  effects on melanomagenesis may be context dependent. PGC1 $\alpha$  controls *MITF* gene expression, contributing to the maintenance of survival in melanomas. Interestingly, peroxisome

proliferator-activated receptor  $\gamma$ , a transcription factor known to bind PGC1 $\alpha$  (Puigserver et al., 1998), regulates *MITF* (Grabacka et al., 2008), suggesting that it might be involved in this process.

These results provide the basis for some potential anticancer therapeutic strategies targeting cellular metabolism. PGC1 $\alpha$ -positive cells depend on PGC1 $\alpha$  for survival, suggesting that PGC1 $\alpha$  itself or one of its target genes could be a therapeutic target. In this regard, although small molecules targeting PGC1 $\alpha$  do not currently exist, inhibitors of estrogen-related receptors (ERRs), key PGC1 transcription factor partners (Mootha et al., 2004; Chang et al., 2011; Schreiber et al., 2004; Eichner and Giguère, 2011; Wende et al., 2005), could potentially be used to inhibit PGC1 $\alpha$  function. Because several transcription factors, including nuclear respiratory factors, ERRs, and YY1 (Scarpulla, 2011; Knutti and Kralli, 2001; Cunningham et al., 2007), control PGC1 $\alpha$  function, future studies will focus to assess which transcription factor(s) partners with PGC1 $\alpha$  to control mitochondrial function and ROS detoxification genes in melanomas. Our data also show that PGC1 $\alpha$ -positive cells are more sensitive to disruption of mitochondrial respiration, suggesting that specific inhibition of respiratory chain complexes could be another vulnerability that could be exploited in this tumor subtype. Importantly, melanoma cells can adapt their metabolism and become PGC1 $\alpha$  independent, underscoring metabolic flexibility as a potential hurdle on developing drugs against metabolic targets. Conversely, PGC1 $\alpha$ -negative melanoma cells have reduced bioenergetic capacity together with lower levels of antioxidant enzymes. As a result, these tumor cells are more sensitive and vulnerable to toxic oxidative stress. This metabolic vulnerability provides a therapeutic strategy to treat this subtype of melanoma tumors (Figure 7). In fact, here we find that ROS-inducing drugs, such as piperlongumine or PEITC, that have been shown to preferentially kill transformed over normal cells (Raj et al., 2011; Trachootham et al., 2006) showed increased potency in PGC1 $\alpha$ -negative melanoma cells.

In summary, our work has revealed that melanoma tumors present heterogeneous metabolic and energetic states defined by levels of PGC1 $\alpha$  expression. These studies illustrate how reprogramming metabolism and energy in tumor cells is genetic dependent and how this information might be used to develop cancer therapy targeting regulatory metabolic networks.

## EXPERIMENTAL PROCEDURES

### Cell Culture and Virus Infection

Melanoma cell lines were cultured in high glucose Dulbecco's modified Eagle's medium supplemented with 10% fetal bovine serum. Immortalized primary melanocytes transduced with pBABE-hygro-*hTERT*, pLNCX2-*CDK4*(R24C), and pBABE-puro-*p53DD* were generated as described (Garraway et al., 2005). Lentiviruses were produced by transfecting HEK293T cells with pLKO and packaging vectors, as previously described (Moffat et al., 2006) using PolyFect (QIAGEN). Retroviral particles were produced by transfecting HEK293T cells with the pBabe or pWZL vectors and packaging vector (pCL-Ampho) using PolyFect (QIAGEN). GFP control and Flag-HA-PGC1 $\alpha$  adenovirus have been previously described (Lerin et al., 2006).

### Animal Studies

All animal studies were performed with an approved protocol from the Beth Israel Deaconess Medical Center Institutional Animal Care and Use Committee

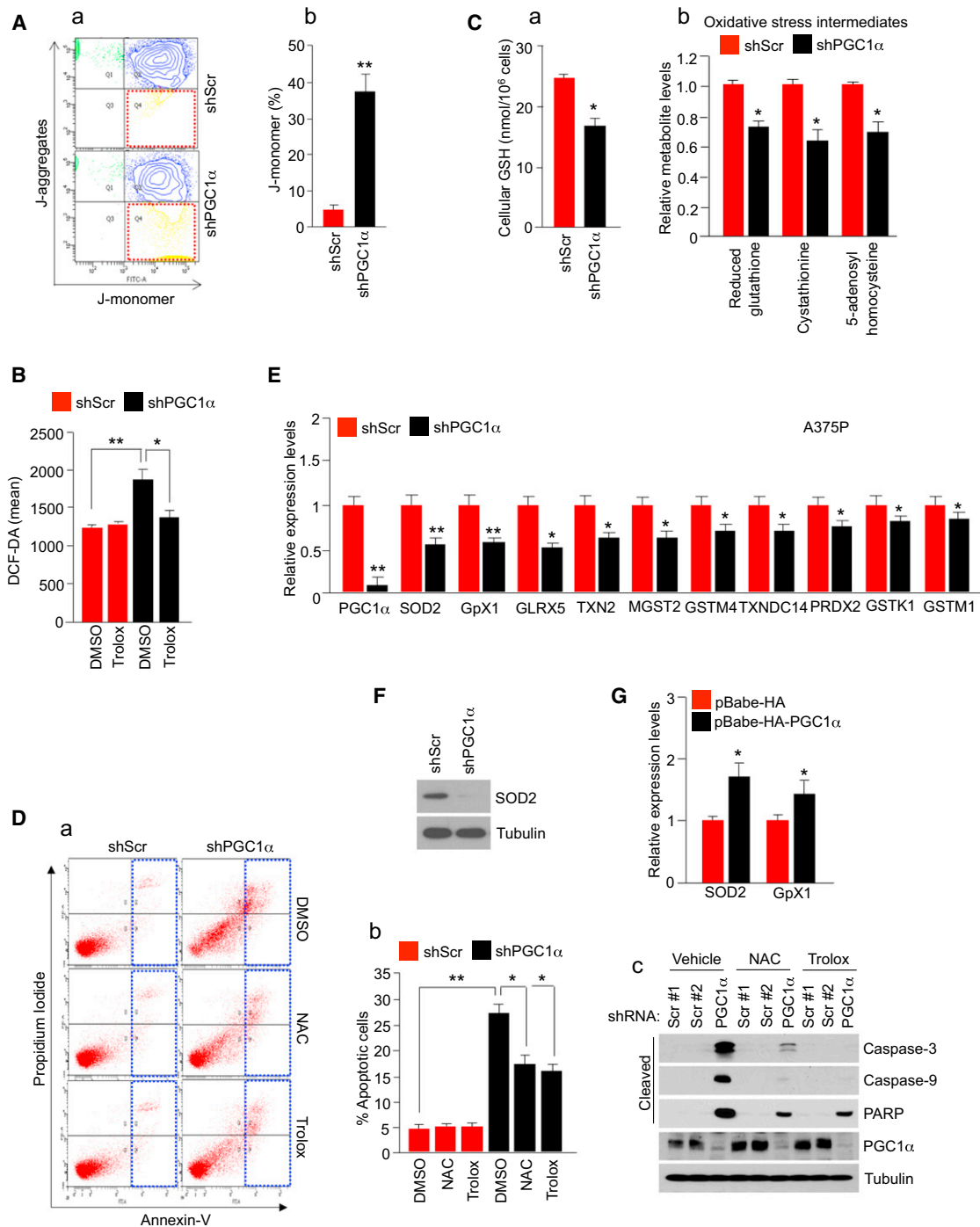


**Figure 5. Depletion of PGC1 $\alpha$  Triggers an Increase in ROS Levels, Causing Apoptosis**

(A) (a) Mitochondrial membrane potential measured by the JC-1 dye in PGC1 $\alpha$  knocked down and control A375P cells. (b) Quantitation of the percentage of J-monomer. Values on the graph represent mean  $\pm$  SD of three independent experiments performed in duplicate. \*\* $p < 0.01$ .

(B) ROS levels in control and PGC1 $\alpha$  knockdown A375P cells measured using the DCF-DA dye. Values represent mean  $\pm$  SD of three independent experiments performed in triplicate. \* $p < 0.05$  and \*\* $p < 0.01$ .

(C) (a) Total GSH levels and (b) oxidative stress intermediates in PGC1 $\alpha$  knocked down and control A375P cells. Values represent mean  $\pm$  SD of three independent experiments performed in triplicate. \* $p < 0.05$ .

(D) Analysis of apoptosis in A375P cells (control and PGC1 $\alpha$  knocked down) treated with 2 mM NAC or 100  $\mu$ M Trolox for 2 days. (a) Annexin V diagram, (b) quantitation of the percentage of apoptotic cells using the Annexin V assay, and (c) western blot analysis of caspases and PARP cleavages. Values on the graph represent mean  $\pm$  SD three independent experiments performed in triplicate. \* $p < 0.05$  and \*\* $p < 0.01$ .

(E) mRNA expression levels of ROS detoxification genes in PGC1 $\alpha$  knockdown A375P melanoma cells. Values represent mean  $\pm$  SD of three independent experiments performed in triplicate. \* $p < 0.05$  and \*\* $p < 0.01$ .

(legend continued on next page)

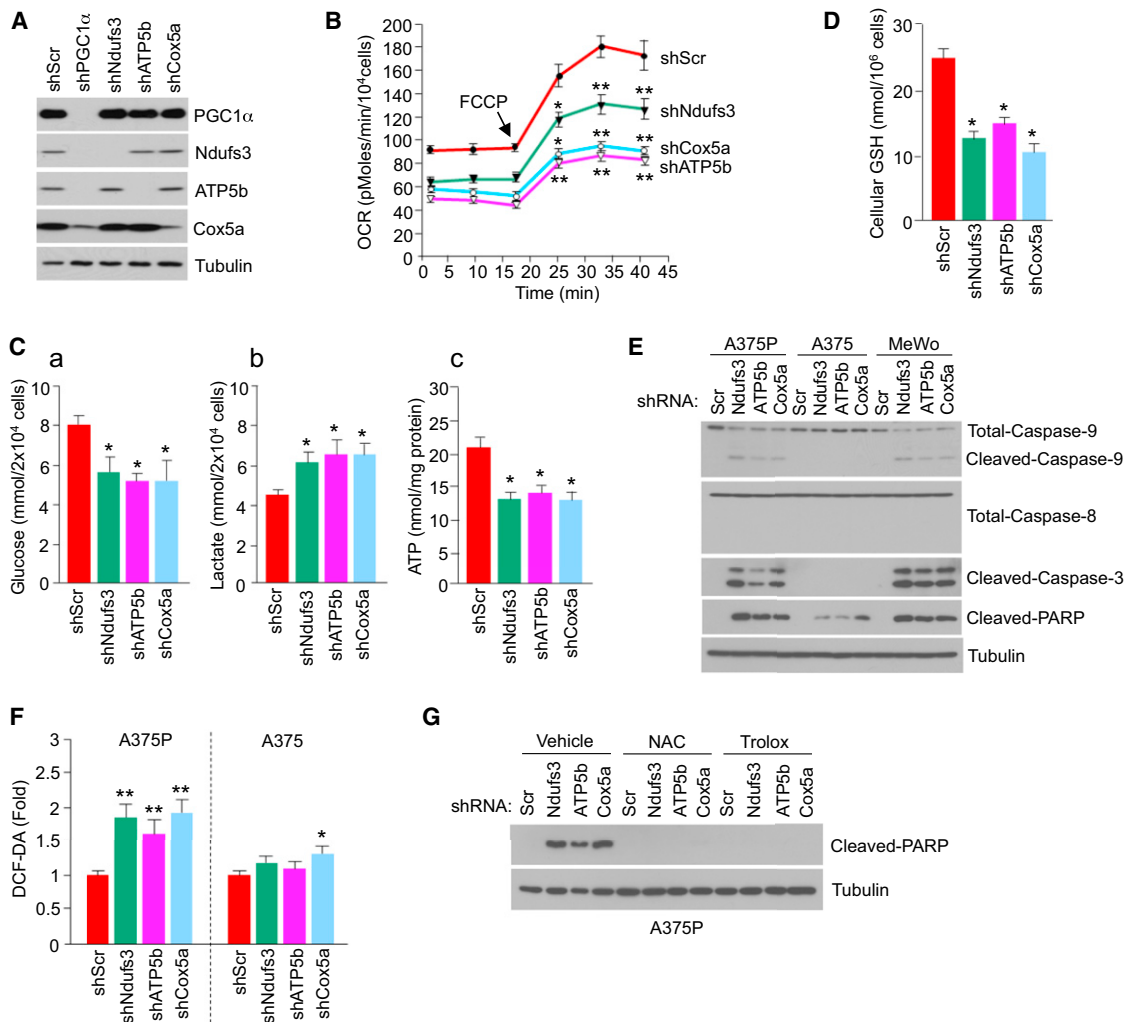


**Figure 6. Induction of ROS-Mediated Apoptosis by Depletion of Mitochondrial Respiration PGC1 $\alpha$  Target Genes**

(A) Depletion of PGC1 $\alpha$  and mitochondrial proteins in A375P melanoma cells.

(B) Real-time measurement of basal and maximal (after addition of FCCP) OCR after knockdown of the indicated genes encoding mitochondrial proteins in A375P. Values represent mean  $\pm$  SD of two independent experiments performed in triplicate. \* $p < 0.05$  and \*\* $p < 0.01$ .

(C) (a) Glucose (in the culture media), (b) lactate (in the culture media), and (c) intracellular ATP levels in A375P after knockdown of the indicated mitochondrial genes. Values represent mean  $\pm$  SD of three independent experiments in duplicate. \* $p < 0.05$ .

(D) Cellular GSH levels in A375P after knockdown of the indicated mitochondrial genes. Values represent mean  $\pm$  SD of three independent experiments in duplicate. \* $p < 0.05$ .

(E) Western blot analysis of apoptotic markers after knockdown of the indicated genes in PGC1 $\alpha$ -positive melanoma cells.

(F) ROS levels, measured by DCF-DA fluorescent dye, after depletion of mitochondrial proteins in A375P or A375 melanoma cells. Values represent mean  $\pm$  SD of three independent experiments in duplicate. \* $p < 0.05$  and \*\* $p < 0.01$ .

(G) Protein expression levels of cleaved PARP after depletion of mitochondrial proteins in A375P melanoma cells treated with the indicated antioxidants.

(Protocol number 105-2011). For xenograft studies,  $1 \times 10^6$  A375P cells stably expressing scrambled shRNA control or PGC1 $\alpha$  shRNA were injected subcutaneously into the flank of nude mice (Taconic) in 100  $\mu$ l of media. After cell injection, mice were incubated for 15 days to allow tumor growth, and then mice were treated with DMSO or piperlongumine (1.5 mg/kg, intraperitoneally [i.p.]) once a day for 6 days. Tumor volumes were measured with a caliper and

calculated using the equation  $\text{volume} = ab^2/2$ , where "a" is the maximal width and "b" is maximal orthogonal width.

#### Arrays and Gene Set Enrichment Analysis

To generate gene-expression arrays, A375P cells were infected with a control shRNA (small hairpin GFP or scrambled short hairpin RNA) or a PGC1 $\alpha$  shRNA

(F) Western blot analysis of SOD2 protein levels in A375P cells.

(G) SOD2 and GpX1 mRNA levels after ectopic expression of PGC1 $\alpha$  in A375 cells. Values represent mean  $\pm$  SD of two independent experiments performed in triplicate. \* $p < 0.05$ .

See also Figure S5.

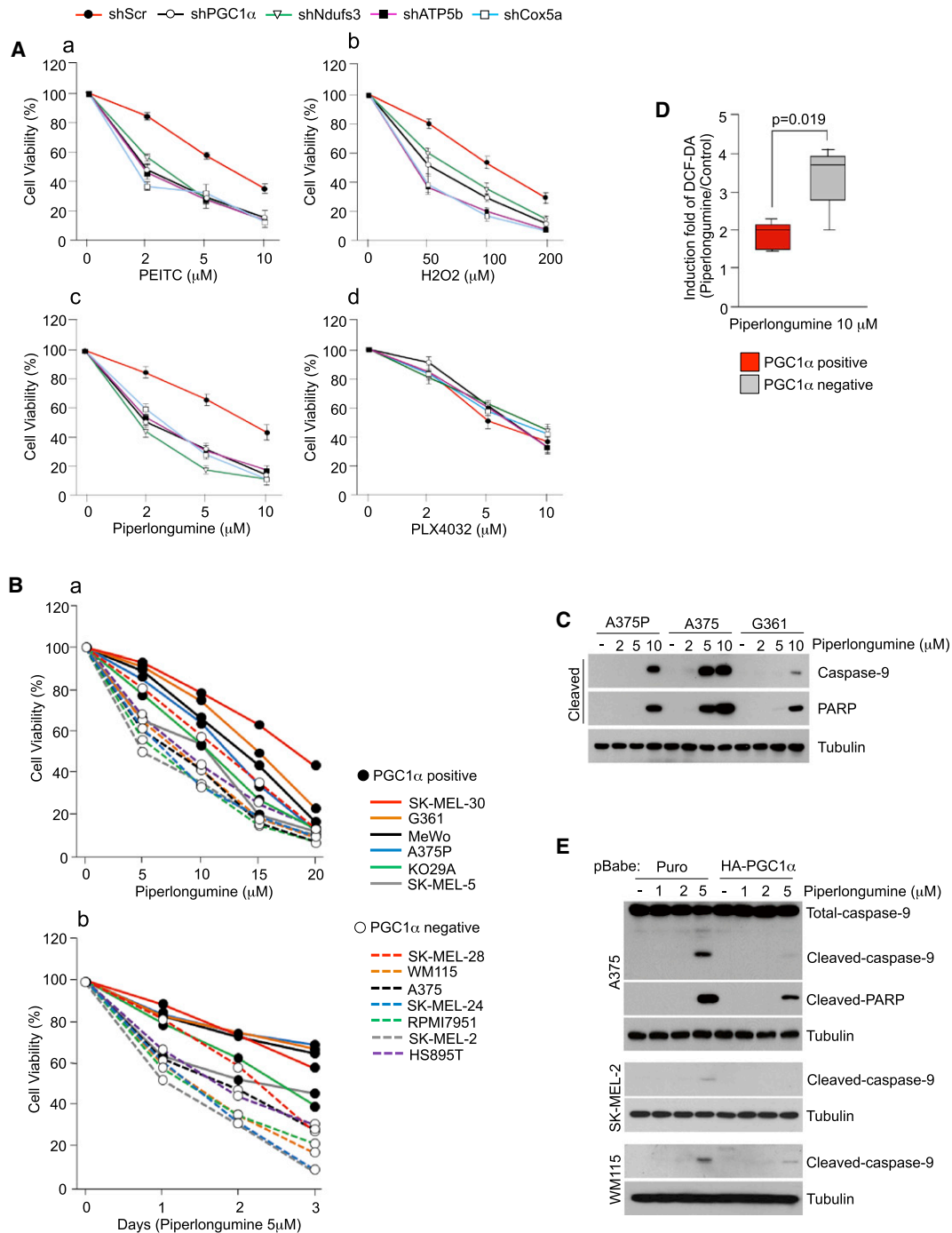


**Figure 7. PGC1 $\alpha$  Expression Decreases Apoptotic Sensitivity to ROS-Inducing Drugs in Human Melanoma Cells**

(A) Cell viability, measured using cell titer glo, after treatment with (a) PEITC, (b) H<sub>2</sub>O<sub>2</sub>, (c) piperlongumine, and (d) PLX4032 in A375P cells stably expressing the indicated shRNAs. Values represent mean  $\pm$  SD of three independent experiments in triplicate.

(B) Cell viability of PGC1 $\alpha$ -positive and negative melanoma cell lines treated with piperlongumine at (a) different concentrations and (b) times. Values represent mean of three independent experiments in triplicate.

(C) Analysis of cleaved caspase-9 and PARP in two PGC1 $\alpha$ -positive (A375P and G361) and one PGC1 $\alpha$ -negative (A375) cell lines treated with piperlongumine.

(D) ROS levels in PGC1 $\alpha$ -positive and -negative melanoma cell lines treated with piperlongumine. Values of three independent experiments performed in duplicate were averaged. The whiskers in the box plots represent the maximum and the minimum value.

(E) Analysis of apoptosis using cleavage of apoptotic markers in PGC1 $\alpha$ -negative melanoma cell lines ectopically expressing PGC1 $\alpha$  and treated with piperlongumine.

See also Figure S6.

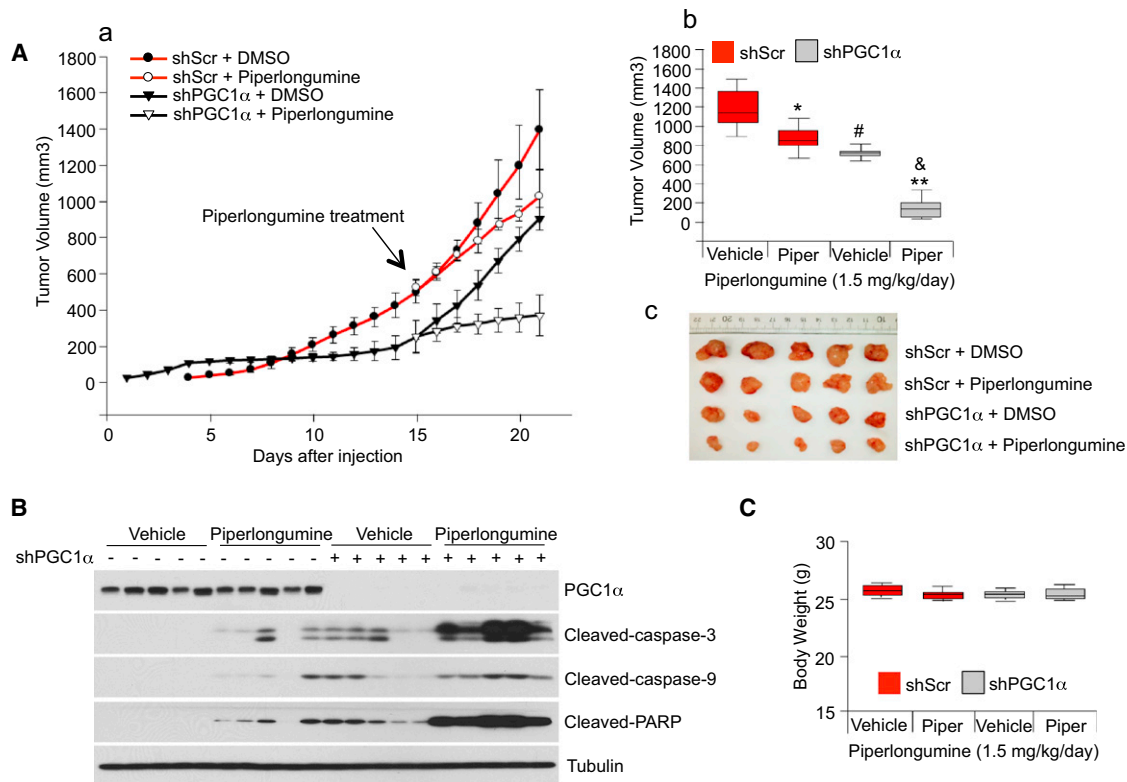


**Figure 8. PGC1 $\alpha$  Expression Decreases Sensitivity to ROS-Inducing Drugs in Human Melanomas**

(A) (a) Tumor volume analysis of xenografts of A375P cells expressing shRNAs against *PGC1 $\alpha$*  or control shRNAs. Fifteen days after cell injection, mice were injected daily with piperlongumine (1.5 mg/kg) or DMSO. The tumor growth curves are plotted as mean  $\pm$  SEM (n = 10, each group). Statistical significance of tumor volumes were calculated by one-way ANOVA with a Tukey posttest; \*p < 0.05; \*\*p < 0.01, DMSO versus piperlongumine; #p < 0.05, DMSO/control shRNA versus DMSO/*PGC1 $\alpha$*  shRNA;  $\delta$ p < 0.01, piperlongumine/control shRNA versus piperlongumine/*PGC1 $\alpha$*  shRNA. (b) In the box plots, final tumor volumes are represented (n = 10). The whiskers in the box plots represent the maximum and the minimum value. (c) Representative images of tumors are shown. (B) Western blot analysis of apoptotic, cleaved caspases and PARP in *PGC1 $\alpha$*  knocked down tumors treated with piperlongumine. (C) Body weight measured at the end of experiment. The whiskers in the box plots represent the maximum and the minimum value.

(described in Supplemental Experimental Procedures) in duplicate and selected with puromycin for 48 hr. Four days after selection, RNA was extracted and gene expression arrays were performed using Human Genome U133A 2.0 arrays. To create a gene expression file, CEL files were used as input for the GenePattern (<http://www.genepattern.broadinstitute.org>) module Expression File Creator using robust multiarray average (RMA) and quantile normalization. The gct file created was used as input for the GSEA analysis.

For the melanoma tumors gene expression analysis, the normalized data set GSE7553 was imported from GEO using the software Gene-e (<http://www.broadinstitute.org/software/gene-e>). The melanoma samples from the data set were selected to create a gct file. This gct file was used as input for the GSEA algorithm.

To find differentially expressed genes, the probes' values were collapsed using maximum average probe and log<sub>2</sub> transformed. The signal to noise marker selection tool from Gene-e was used to find genes differentially expressed between the top and the bottom 25% *PGC1 $\alpha$* -expressing melanoma tumors with 10,000 permutations. The cutoff to select the gene list was fold change >2, false discovery rate (FDR) q < 0.25. For the melanoma cell lines gene expression analysis, the gene-centric RMA-normalized CCLE expression data set was used (<http://www.broadinstitute.org/ccle>).

The GSEA software v2.0 (<http://www.broadinstitute.org/gsea>; Subramanian et al., 2005) was used to perform the GSEA analysis. In all the analysis, the Reactome gene sets were used and the number of permutations was changed to 5,000. For the GSEA7553 slice data set, the values of the 219195\_at probe (corresponding to *PPARGC1A*) were used as phenotype and the default parameters were used with the exception that Pearson correlation

was computed to rank the genes. For the analysis of the A375P data set, the default parameters were used but the permutation type was changed to gene set.

#### Oxygen Consumption

The oxygen consumption rate was measured using an optical fluorescent oxygen sensor in a Seahorse Bioscience XF24 Extracellular Flux Analyzer. Briefly, cells were seeded in quadruplicate at equal densities (25,000 cells per well) into XF24 tissue culture plates. Cell media was changed 12 hr after cell seeding into unbuffered Dulbecco's modified Eagle's medium (DMEM) (8.3 g/l DMEM [Sigma], 200 mM GlutaMax-1 [Invitrogen], 25 mM D-glucose [Sigma], 63.3 mM NaCl [Sigma], and phenol red [Sigma], adjusted pH to 7.4 with NaOH), according to the manufacturer's protocol. Oxygen consumption was measured under basal conditions and mitochondrial uncoupler trifluoromethoxy carbonyl cyanide phenyl hydrazone (FCCP) (2  $\mu$ M). Oxygen consumption values were normalized to cell number.

#### Intracellular ROS and Cellular GSH Levels

To measure intracellular ROS levels, 2  $\mu$ M dichlorofluorescein diacetate (DCF-DA) (Invitrogen) was used as a fluorescent dye. An equal number of cells were seeded in six well plates, after 72 hr cells were trypsinized, washed once with PBS, and stained with DCF-DA in Hank's balanced salt solution for 30 min at 37°C. Samples were then immediately analyzed by flow cytometry.

A glutathione colorimetric detection kit (BioVision Research Products) was used to measure total cellular glutathione according to the manufacturer's instructions.

## ACCESSION NUMBERS

The Gene Expression Omnibus accession number for the gene expression data reported is GSE36879.

## SUPPLEMENTAL INFORMATION

Supplemental Information includes six figures, three tables, and Supplemental Experimental Procedures and can be found with this article online at <http://dx.doi.org/10.1016/j.ccr.2012.11.020>.

## ACKNOWLEDGMENTS

We thank the Dana-Farber Cancer Institute Microarray Core Facility for performing the gene-expression arrays and the Dana-Farber RNAi facility for the shRNA constructs. These studies were funded by the Claudia Adams Barr Program in Cancer Research and Dana-Farber Cancer Institute funds. H.R.W. acknowledges support from P50CA093683.

Received: March 30, 2012

Revised: August 3, 2012

Accepted: November 30, 2012

Published: February 14, 2013

## REFERENCES

- Barretina, J., Caponigro, G., Stransky, N., Venkatesan, K., Margolin, A.A., Kim, S., Wilson, C.J., Lehár, J., Kryukov, G.V., Sonkin, D., et al. (2012). The Cancer Cell Line Encyclopedia enables predictive modelling of anticancer drug sensitivity. *Nature* **483**, 603–607.
- Bertolotto, C., Lesueur, F., Giuliano, S., Strub, T., de Lichy, M., Bille, K., Dessen, P., d'Hayer, B., Mohamdi, H., Remenieras, A., et al.; French Familial Melanoma Study Group (2011). A SUMOylation-defective MITF germline mutation predisposes to melanoma and renal carcinoma. *Nature* **480**, 94–98.
- Bogunovic, D., O'Neill, D.W., Belitskaya-Levy, I., Vacic, V., Yu, Y.L., Adams, S., Darvishian, F., Berman, R., Shapiro, R., Pavlick, A.C., et al. (2009). Immune profile and mitotic index of metastatic melanoma lesions enhance clinical staging in predicting patient survival. *Proc. Natl. Acad. Sci. USA* **106**, 20429–20434.
- Chang, C.Y., Kazmin, D., Jasper, J.S., Kunder, R., Zuercher, W.J., and McDonnell, D.P. (2011). The metabolic regulator ERR $\alpha$ , a downstream target of HER2/IGF-1R, as a therapeutic target in breast cancer. *Cancer Cell* **20**, 500–510.
- Choo, A.Y., Kim, S.G., Vander Heiden, M.G., Mahoney, S.J., Vu, H., Yoon, S.O., Cantley, L.C., and Blenis, J. (2010). Glucose addiction of TSC null cells is caused by failed mTORC1-dependent balancing of metabolic demand with supply. *Mol. Cell* **38**, 487–499.
- Clark, E.A., Golub, T.R., Lander, E.S., and Hynes, R.O. (2000). Genomic analysis of metastasis reveals an essential role for RhoC. *Nature* **406**, 532–535.
- Cunningham, J.T., Rodgers, J.T., Arlow, D.H., Vazquez, F., Mootha, V.K., and Puigserver, P. (2007). mTOR controls mitochondrial oxidative function through a YY1-PGC-1 $\alpha$  transcriptional complex. *Nature* **450**, 736–740.
- Diehn, M., Cho, R.W., Lobo, N.A., Kalisky, T., Dorie, M.J., Kulp, A.N., Qian, D., Lam, J.S., Ailles, L.E., Wong, M., et al. (2009). Association of reactive oxygen species levels and radioresistance in cancer stem cells. *Nature* **458**, 780–783.
- Eichner, L.J., and Giguère, V. (2011). Estrogen related receptors (ERRs): a new dawn in transcriptional control of mitochondrial gene networks. *Mitochondrion* **11**, 544–552.
- Fernandez-Marcos, P.J., and Auwerx, J. (2011). Regulation of PGC-1 $\alpha$ , a nodal regulator of mitochondrial biogenesis. *Am. J. Clin. Nutr.* **93**, 884S–890S.
- Gao, P., Tchernyshyov, I., Chang, T.C., Lee, Y.S., Kita, K., Ochi, T., Zeller, K.I., De Marzo, A.M., Van Eyk, J.E., Mendell, J.T., and Dang, C.V. (2009). c-Myc suppression of miR-23a/b enhances mitochondrial glutaminase expression and glutamine metabolism. *Nature* **458**, 762–765.
- Garraway, L.A., Widlund, H.R., Rubin, M.A., Getz, G., Berger, A.J., Ramaswamy, S., Beroukhi, R., Milner, D.A., Granter, S.R., Du, J., et al. (2005). Integrative genomic analyses identify MITF as a lineage survival oncogene amplified in malignant melanoma. *Nature* **436**, 117–122.
- Grabacka, M., Placha, W., Urbanska, K., Laidler, P., Plonka, P.M., and Reiss, K. (2008). PPAR gamma regulates MITF and beta-catenin expression and promotes a differentiated phenotype in mouse melanoma S91. *Pigment Cell Melanoma Res.* **21**, 388–396.
- Hanahan, D., and Weinberg, R.A. (2011). Hallmarks of cancer: the next generation. *Cell* **144**, 646–674.
- Handschin, C., Chin, S., Li, P., Liu, F., Maratos-Flier, E., Lebrasseur, N.K., Yan, Z., and Spiegelman, B.M. (2007). Skeletal muscle fiber-type switching, exercise intolerance, and myopathy in PGC-1 $\alpha$  muscle-specific knock-out animals. *J. Biol. Chem.* **282**, 30014–30021.
- Herzig, S., Long, F., Jhala, U.S., Hedrick, S., Quinn, R., Bauer, A., Rudolph, D., Schutz, G., Yoon, C., Puigserver, P., et al. (2001). CREB regulates hepatic gluconeogenesis through the coactivator PGC-1. *Nature* **413**, 179–183.
- Hoek, K.S., Eichhoff, O.M., Schlegel, N.C., Döbbeling, U., Kobert, N., Schaerer, L., Hemmi, S., and Dummer, R. (2008). In vivo switching of human melanoma cells between proliferative and invasive states. *Cancer Res.* **68**, 650–656.
- Kelly, D.P., and Scarpulla, R.C. (2004). Transcriptional regulatory circuits controlling mitochondrial biogenesis and function. *Genes Dev.* **18**, 357–368.
- Knutti, D., and Kralli, A. (2001). PGC-1, a versatile coactivator. *Trends Endocrinol. Metab.* **12**, 360–365.
- Lerin, C., Rodgers, J.T., Kalume, D.E., Kim, S.H., Pandey, A., and Puigserver, P. (2006). GCN5 acetyltransferase complex controls glucose metabolism through transcriptional repression of PGC-1 $\alpha$ . *Cell Metab.* **3**, 429–438.
- Lin, J., Wu, H., Tarr, P.T., Zhang, C.Y., Wu, Z., Boss, O., Michael, L.F., Puigserver, P., Isotani, E., Olson, E.N., et al. (2002). Transcriptional coactivator PGC-1 $\alpha$  drives the formation of slow-twitch muscle fibres. *Nature* **418**, 797–801.
- Lin, W.M., Baker, A.C., Beroukhi, R., Winckler, W., Feng, W., Marmion, J.M., Laine, E., Greulich, H., Tseng, H., Gates, C., et al. (2008). Modeling genomic diversity and tumor dependency in malignant melanoma. *Cancer Res.* **68**, 664–673.
- Moffat, J., Grueneberg, D.A., Yang, X., Kim, S.Y., Kloepfer, A.M., Hinkle, G., Piqui, B., Eisenhaure, T.M., Luo, B., Grenier, J.K., et al. (2006). A lentiviral RNAi library for human and mouse genes applied to an arrayed viral high-content screen. *Cell* **124**, 1283–1298.
- Mootha, V.K., Lindgren, C.M., Eriksson, K.F., Subramanian, A., Sihag, S., Lehar, J., Puigserver, P., Carlsson, E., Ridderstråle, M., Laurila, E., et al. (2003). PGC-1 $\alpha$ -responsive genes involved in oxidative phosphorylation are coordinately downregulated in human diabetes. *Nat. Genet.* **34**, 267–273.
- Mootha, V.K., Handschin, C., Arlow, D., Xie, X., St Pierre, J., Sihag, S., Yang, W., Altshuler, D., Puigserver, P., Patterson, N., et al. (2004). Erralpha and Galpha/b specify PGC-1 $\alpha$ -dependent oxidative phosphorylation gene expression that is altered in diabetic muscle. *Proc. Natl. Acad. Sci. USA* **101**, 6570–6575.
- Ohta, T., Iijima, K., Miyamoto, M., Nakahara, I., Tanaka, H., Ohtsuji, M., Suzuki, T., Kobayashi, A., Yokota, J., Sakiyama, T., et al. (2008). Loss of Keap1 function activates Nrf2 and provides advantages for lung cancer cell growth. *Cancer Res.* **68**, 1303–1309.
- Padmanabhan, B., Tong, K.I., Ohta, T., Nakamura, Y., Scharlock, M., Ohtsuji, M., Kang, M.I., Kobayashi, A., Yokoyama, S., and Yamamoto, M. (2006). Structural basis for defects of Keap1 activity provoked by its point mutations in lung cancer. *Mol. Cell* **21**, 689–700.
- Puigserver, P., and Spiegelman, B.M. (2003). Peroxisome proliferator-activated receptor-gamma coactivator 1 alpha (PGC-1 alpha): transcriptional coactivator and metabolic regulator. *Endocr. Rev.* **24**, 78–90.
- Puigserver, P., Wu, Z., Park, C.W., Graves, R., Wright, M., and Spiegelman, B.M. (1998). A cold-inducible coactivator of nuclear receptors linked to adaptive thermogenesis. *Cell* **92**, 829–839.

- Raj, L., Ide, T., Gurkar, A.U., Foley, M., Schenone, M., Li, X., Tolliday, N.J., Golub, T.R., Carr, S.A., Shamji, A.F., et al. (2011). Selective killing of cancer cells by a small molecule targeting the stress response to ROS. *Nature* *475*, 231–234.
- Rhee, J., Inoue, Y., Yoon, J.C., Puigserver, P., Fan, M., Gonzalez, F.J., and Spiegelman, B.M. (2003). Regulation of hepatic fasting response by PPARgamma coactivator-1alpha (PGC-1): requirement for hepatocyte nuclear factor 4alpha in gluconeogenesis. *Proc. Natl. Acad. Sci. USA* *100*, 4012–4017.
- Riker, A.I., Enkemann, S.A., Fodstad, O., Liu, S., Ren, S., Morris, C., Xi, Y., Howell, P., Metge, B., Samant, R.S., et al. (2008). The gene expression profiles of primary and metastatic melanoma yields a transition point of tumor progression and metastasis. *BMC Med. Genomics* *1*, 13.
- Sahin, E., Colla, S., Liesa, M., Moslehi, J., Müller, F.L., Guo, M., Cooper, M., Kotton, D., Fabian, A.J., Walkey, C., et al. (2011). Telomere dysfunction induces metabolic and mitochondrial compromise. *Nature* *470*, 359–365.
- Scarpulla, R.C. (2011). Metabolic control of mitochondrial biogenesis through the PGC-1 family regulatory network. *Biochim. Biophys. Acta* *1813*, 1269–1278.
- Schreiber, S.N., Emter, R., Hock, M.B., Knutti, D., Cardenas, J., Podvinec, M., Oakeley, E.J., and Kralli, A. (2004). The estrogen-related receptor alpha (ERRalpha) functions in PPARgamma coactivator 1alpha (PGC-1alpha)-induced mitochondrial biogenesis. *Proc. Natl. Acad. Sci. USA* *101*, 6472–6477.
- Sen, N., Satija, Y.K., and Das, S. (2011). PGC-1 $\alpha$ , a key modulator of p53, promotes cell survival upon metabolic stress. *Mol. Cell* *44*, 621–634.
- Shibata, T., Ohta, T., Tong, K.I., Kokubu, A., Odogawa, R., Tsuta, K., Asamura, H., Yamamoto, M., and Hirohashi, S. (2008). Cancer related mutations in NRF2 impair its recognition by Keap1-Cul3 E3 ligase and promote malignancy. *Proc. Natl. Acad. Sci. USA* *105*, 13568–13573.
- Singh, A., Misra, V., Thimmulappa, R.K., Lee, H., Ames, S., Hoque, M.O., Herman, J.G., Baylin, S.B., Sidransky, D., Gabrielson, E., et al. (2006). Dysfunctional KEAP1-NRF2 interaction in non-small-cell lung cancer. *PLoS Med.* *3*, e420.
- St-Pierre, J., Drori, S., Uldry, M., Silvaggi, J.M., Rhee, J., Jäger, S., Handschin, C., Zheng, K., Lin, J., Yang, W., et al. (2006). Suppression of reactive oxygen species and neurodegeneration by the PGC-1 transcriptional coactivators. *Cell* *127*, 397–408.
- Strub, T., Giuliano, S., Ye, T., Bonet, C., Keime, C., Kobi, D., Le Gras, S., Cormont, M., Ballotti, R., Bertolotto, C., and Davidson, I. (2011). Essential role of microphthalmia transcription factor for DNA replication, mitosis and genomic stability in melanoma. *Oncogene* *30*, 2319–2332.
- Subramanian, A., Tamayo, P., Mootha, V.K., Mukherjee, S., Ebert, B.L., Gillette, M.A., Paulovich, A., Pomeroy, S.L., Golub, T.R., Lander, E.S., and Mesirov, J.P. (2005). Gene set enrichment analysis: a knowledge-based approach for interpreting genome-wide expression profiles. *Proc. Natl. Acad. Sci. USA* *102*, 15545–15550.
- Tait, S.W., and Green, D.R. (2010). Mitochondria and cell death: outer membrane permeabilization and beyond. *Nature Rev. Mol. Cell Biol.* *11*, 621–632.
- Trachootham, D., Zhou, Y., Zhang, H., Demizu, Y., Chen, Z., Pelicano, H., Chiao, P.J., Achanta, G., Arlinghaus, R.B., Liu, J., and Huang, P. (2006). Selective killing of oncogenically transformed cells through a ROS-mediated mechanism by beta-phenylethyl isothiocyanate. *Cancer Cell* *10*, 241–252.
- Trachootham, D., Alexandre, J., and Huang, P. (2009). Targeting cancer cells by ROS-mediated mechanisms: a radical therapeutic approach? *Nat. Rev. Drug Discov.* *8*, 579–591.
- Weinberg, F., and Chandel, N.S. (2009). Mitochondrial metabolism and cancer. *Ann. N Y Acad. Sci.* *1177*, 66–73.
- Wende, A.R., Huss, J.M., Schaeffer, P.J., Giguère, V., and Kelly, D.P. (2005). PGC-1alpha coactivates PDK4 gene expression via the orphan nuclear receptor ERRalpha: a mechanism for transcriptional control of muscle glucose metabolism. *Mol. Cell. Biol.* *25*, 10684–10694.
- Wise, D.R., DeBerardinis, R.J., Mancuso, A., Sayed, N., Zhang, X.Y., Pfeiffer, H.K., Nissim, I., Daikhin, E., Yudkoff, M., McMahon, S.B., and Thompson, C.B. (2008). Myc regulates a transcriptional program that stimulates mitochondrial glutaminolysis and leads to glutamine addiction. *Proc. Natl. Acad. Sci. USA* *105*, 18782–18787.
- Yokoyama, S., Woods, S.L., Boyle, G.M., Aoude, L.G., MacGregor, S., Zismann, V., Gartside, M., Cust, A.E., Haq, R., Harland, M., et al. (2011). A novel recurrent mutation in MITF predisposes to familial and sporadic melanoma. *Nature* *480*, 99–103.
- Zaugg, K., Yao, Y., Reilly, P.T., Kannan, K., Kiarash, R., Mason, J., Huang, P., Sawyer, S.K., Fuerth, B., Faubert, B., et al. (2011). Carnitine palmitoyltransferase 1C promotes cell survival and tumor growth under conditions of metabolic stress. *Genes Dev.* *25*, 1041–1051.